

# Period-Luminosity Relations for Type II Cepheids and their Application

Noriyuki Matsunaga<sup>1\*</sup>, Michael W. Feast<sup>2,3</sup>, and John W. Menzies<sup>3</sup>

<sup>1</sup> Department of Astronomy, Kyoto University, Kitashirakawa-Oiwake-cho, Sakyo-ku, Kyoto 606-8502, Japan;

Research Fellow of the Japan Society for the Promotion of Science

<sup>2</sup> Department of Astronomy, University of Cape Town, 7701, Rondebosch, South Africa

<sup>3</sup> South African Astronomical Observatory, PO Box 9, 7935, Observatory, South Africa

Accepted 29 April 2009. Received 29 April 2009; in original form 24 March 2009

## ABSTRACT

$JHK_s$  magnitudes corrected to mean intensity are estimated for LMC type II Cepheids in the OGLE-III survey. Period-luminosity (PL) relations are derived in  $JHK_s$  as well as in a reddening-free  $VI$  parameter. Within the uncertainties the BL Her stars ( $P < 4$  d) and the W Vir stars ( $P = 4$  to 20 d) are co-linear in these PL relations. The slopes of the infrared relations agree with those found previously for type II Cepheids in globular clusters within the uncertainties. Using the pulsation parallaxes of V553 Cen and SW Tau the data lead to an LMC modulus uncorrected for any metallicity effects of  $18.46 \pm 0.10$  mag. The type II Cepheids in the second-parameter globular cluster, NGC 6441, show a  $PL(VI)$  relation of the same slope as that in the LMC and this leads to a cluster distance modulus of  $15.46 \pm 0.11$  mag, confirming the hypothesis that the RR Lyrae variables in this cluster are overluminous for their metallicity. It is suggested that the Galactic variable  $\kappa$  Pav is a member of the peculiar W Vir class found by the OGLE-III group in the LMC. Low-resolution spectra of OGLE-III type II Cepheids with  $P > 20$  d (RV Tau stars) show that a high proportion have TiO bands; only one has been found showing  $C_2$ . The LMC RV Tau stars, as a group, are not co-linear with the shorter-period type II Cepheids in the infrared PL relations in marked contrast to such stars in globular clusters. Other differences between LMC, globular cluster and Galactic field type II Cepheids are noted in period distribution and infrared colours.

**Key words:** stars: distances – stars: Population II – stars: variables Cepheids – stars: variables: other – galaxies: Magellanic Clouds – infrared: stars.

## 1 INTRODUCTION

Type II Cepheids (Cepheids) have periods in the same range as classical Cepheids but are lower-mass stars belonging to disc and halo populations. They are conventionally divided into three period groups; BL Her stars (BL) at short periods, W Vir stars (WV) at intermediate periods, and RV Tau stars (RV) at the longest periods. The period divisions tend to be somewhat arbitrary. In a recent paper to which considerable reference will be made, Soszyński et al. (2008, hereafter S08) adopt divisions at 4 and 20 d, and we follow these thresholds here. The RV stars tend to show alternating deep and shallow minima (and this is often taken as a defining characteristic), but the single period of the RVs will be used in this paper as in S08. In addition to the BL, WV, and RV stars, S08 define an ad-

ditional class of peculiar W Vir (pW) stars which will be discussed below.

Most workers have accepted the evolutionary scheme elaborated by Gingold (1976, 1985). In this the BL stars are evolving from the (blue) horizontal branch towards the lower asymptotic giant branch (AGB). The WV stars are on loops to the blue from the AGB and the RV stars are moving to the blue in a post-AGB phase. Matsunaga et al. (2006, hereafter M06) showed that the Cepheids in globular clusters defined narrow period-luminosity (PL) relations in the near-infrared bands,  $JHK_s$ , with little evidence for a metallicity effect in these relations. This suggests that these stars may be useful distance indicators for disc and halo populations. Pulsation parallaxes of Galactic Cepheids were used by Feast et al. (2008, hereafter F08) to calibrate these cluster PL relations and to discuss the distances of the LMC and the Galactic centre.

The present paper discusses the Cepheids in the LMC based on the recent optical OGLE-III survey (S08) and the results of the near-infrared survey with the Infrared Survey Facility (IRSF). The Cepheids in the second-parameter cluster NGC 6441 and those

\* An e-mail address and the current address of NM are as follows: matsunaga@ioa.s.u-tokyo.ac.jp, Institute of Astronomy, University of Tokyo, 2-21-1 Osawa, Mitaka, Tokyo 181-0015, Japan

around the Galactic centre are also discussed as well as the nature of the CephII variable  $\kappa$  Pav.

## 2 INFRARED PHOTOMETRY

S08 catalogued 197 CephII variables in the LMC. We searched for near-infrared counterparts in the IRSF catalogue (Kato et al. 2007). This is a point-source catalogue in  $JHK_s$  of  $40 \text{ deg}^2$  of the LMC,  $11 \text{ deg}^2$  of the SMC, and  $4 \text{ deg}^2$  of the Magellanic Bridge. The catalogue is based on simultaneous images in  $JHK_s$  obtained with the 1.4-m IRSF telescope and the Simultaneous 3-colour Infrared Imager for Unbiased Survey (SIRIUS) based at the South African Astronomical Observatory (SAAO), Sutherland. The  $10 \sigma$  limiting magnitudes of the survey are 18.8, 17.8 and 16.6 mag  $J$ ,  $H$ , and  $K_s$ . The catalogue reaches fainter and has higher resolution than the point-source catalogue of the 2 Micron All Sky Survey (2MASS, Skrutskie et al. 2006) in the region of the Magellanic Clouds.

We found matches for 188 S08 CephII sources with a tolerance of 0.5 arcsec. The differences in coordinate are small between the catalogues with a standard deviation of less than 0.1 arcsec in both Right Ascension and Declination. Among nine sources without IRSF counterparts, seven (1–3, 194–197) are located outside of the IRSF survey field. There are no counterparts around the two BL stars (69 and 123) probably because they are too faint. These variables actually have the shortest periods among our sample. On the other hand, we found two IRSF counterparts for 15 S08 sources: these IRSF counterparts were detected in neighbouring fields of the IRSF survey as listed in Table 1.

IRSF magnitudes in all three bands are not available for nine BLs and one pW. In most of the cases,  $K_s$ -band magnitudes are missing because of the faintness of the short-period BLs.  $H$ -band magnitudes are unavailable for No. 40 (pW) and 144 (BL); the reason for this is unclear.

Since S08 give the periods and dates of maximum light in  $I$  (= phase zero), we can derive the phases (between zero and one) of the single  $JHK_s$  observations. Using the  $I$ -band light curves we obtain the value of  $I$  at that phase and its difference from the intensity mean value,  $\langle I \rangle$ . Assuming that the light curves in  $JHK_s$  are similar to those in  $I$ , we obtain an estimate of the mean (phase-corrected) magnitude in each infrared band.

In order to check the validity of the above assumption, we use the S08 sources with two IRSF counterparts. There are 15 such sources (2 RV, 7 WV, 6 BL). We list the dates, phases, and observed magnitudes from the two IRSF measurements in Table 1. For each phase at which the IRSF survey was conducted, we also estimate a predicted  $I$ -band magnitude by taking a mean of the  $I$ -band measurements which were made within  $\pm 0.05$  of the phase of the IRSF survey. Variations between two IRSF measurements ( $\Delta J$ ,  $\Delta H$ ,  $\Delta K_s$ ) have the same signs as the difference between the predicted  $I$ -band magnitudes ( $\Delta I$ ) for each object. Fig. 1 plots the variations of the IRSF measurements against  $\Delta I$ . This clearly shows the variations in  $JHK_s$  reasonably agree with those in  $I$ , except for the  $\Delta K_s$  values for BLs (crosses) which have large error bars. That is, these observations are consistent with the assumption that the  $JHK_s$  light curves are, to a first approximation, similar to those at  $I$  and have about the same amplitude.

Light curves of RV stars often have a large scatter, and it is difficult to make satisfactory phase corrections. We selected eight RVs which have good light curves, i.e. 5, 58, 104, 115, 125, 135, 169, and 192, and use these light curves to make phase corrections.

For pW, we do not try to correct the phase effect, and they are not included in the following discussions of the PL relation.

We here present a catalogue of the S08 sources with the IRSF counterparts in Table 2, where the  $JHK_s$  values are those listed in the IRSF catalogue (Kato et al. 2007). The indicated errors,  $E_J$ ,  $E_H$ , and  $E_K$ , are taken from their catalogue. The quantity  $\delta_\phi$  is the correction which must be added to the  $I$  magnitude at the epoch of the IRSF observation to correct it to the intensity mean magnitude and is the value we adopt to correct the infrared magnitudes to means. Note that we list those with two IRSF counterparts in neighbouring fields twice.

## 3 PERIOD-LUMINOSITY RELATIONS

### 3.1 General and Optical Relations

In this section we discuss the optical PL relations using the data in S08. Based on notes given by S08 the following stars were omitted in all solutions, optical and infrared; 88, 153, 166, 185 (blends); 21, 23, 52, 77, 84, 93, 98 (eclipsing), 50 (too blue), 108 (low amplitude), 113 (scatter in light curve), 51 (variable amplitude), and 150 (variable mean magnitude).

The general features of CephII optical period-luminosity diagrams are well shown in fig. 1 of S08. The plots of  $V$  and  $I$  against  $\log P$  show considerable scatter and clear non-linearity. Introduction of a colour term [ $W = I - R(V - I)$ ] with  $R = 1.55$  produces a rather narrow and nearly linear PL( $W$ ) relation for the BL and WV stars although there is still scatter amongst the RVs.

S08 recognize a class of peculiar W Vir (pW) stars. These have distinctive light curves and a high proportion are binaries. Many of these lie above (brighter than) the normal WV stars in the various PL plots. In the solutions below all the pW stars are omitted. There are also a few stars in the BL period range which in the PL( $W$ ) plot lie brighter than the bulk of the BL stars and in the region occupied by anomalous Cepheids. We have chosen to omit these stars (107, 114, 142, 153, 166) in our work.

If the value of  $R$  is correctly chosen,  $W$  is a reddening-free parameter. Udalski et al. (1999) found  $R = 1.55$  as appropriate to the OGLE-II photometry from the results of Schlegel, Finkbeiner, & Davis (1998). On the other hand, a value of  $R = 1.45$  has frequently been used (e.g. Freedman et al. 2001; van Leeuwen et al. 2007). This latter value is based on the extinction law of Cardelli, Clayton, & Mathis (1989). We give below results based on both values of  $R$ . In work with very heavily reddened stars the exact value of  $R$  may become important.

For 55 BL stars we find:

$$W_1 = I - 1.55(V - I) = -2.598(\pm 0.094)(\log P - 0.3) + 16.597(\pm 0.017), (\sigma = 0.104), \quad (1)$$

and

$$W_2 = I - 1.45(V - I) = -2.572(\pm 0.093)(\log P - 0.3) + 16.665(\pm 0.016), (\sigma = 0.103). \quad (2)$$

For 76 WV stars we find:

$$W_3 = I - 1.55(V - I) = -2.564(\pm 0.073)(\log P - 1.2) + 14.333(\pm 0.019), (\sigma = 0.108), \quad (3)$$

and

$$W_4 = I - 1.45(V - I) = -2.551(\pm 0.073)(\log P - 1.2) + 14.431(\pm 0.019), (\sigma = 0.105). \quad (4)$$

**Table 1.** The LMC Cepheids with two IRSF measurements. Modified Julian Dates (MJD), pulsation phase of the observations, and  $JHK_s$  magnitudes and their errors are listed for each IRSF entry. Also indicated are  $I$ -band magnitudes at the phases of the IRSF measurements based on the OGLE light curves.

OGLE-ID	Type	log $P$	IRSF-Field		IRSF counterpart							Expected $I$
			IRSF-Field	MJD(obs)	Phase	$J$	$E_J$	$H$	$E_H$	$K_s$	$E_K$	
10	BLHer	0.17695	LMC0456-6840I	53062.869	0.681	17.71	0.04	17.35	0.04	17.23	0.25	18.26
10			LMC0452-6840G	53049.895	0.049	17.33	0.03	17.06	0.04	16.90	0.17	17.70
11	RVTau	1.59391	LMC0453-6740G	52683.765	0.578	13.71	0.03	13.32	0.03	13.25	0.02	14.17
11			LMC0454-6720A	53017.960	0.091	13.42	0.01	13.12	0.01	13.03	0.02	14.03
22	WVir	1.03006	LMC0458-7040G	53497.695	0.076	15.44	0.02	15.05	0.02	15.04	0.03	16.13
22			LMC0502-7040I	53117.759	0.623	15.75	0.02	15.34	0.02	15.29	0.03	16.38
38	WVir	0.60354	LMC0503-6840A	53123.751	0.964	15.94	0.02	15.87	0.02	15.84	0.05	16.10
38			LMC0507-6840C	53341.916	0.320	15.85	0.01	15.66	0.02	15.66	0.05	16.09
50	RVTau	1.54093	LMC0511-6840C	53051.855	0.304	14.35	0.02	14.03	0.02	13.82	0.02	14.93
50			LMC0511-6900I	52612.916	0.672	14.65	0.03	14.30	0.02	14.10	0.02	15.07
59	WVir	1.22365	LMC0510-7040G	53322.877	0.012	14.68	0.01	14.36	0.01	14.22	0.02	15.28
59			LMC0514-7040I	52714.762	0.677	15.42	0.02	15.05	0.02	15.01	0.04	15.90
76	BLHer	0.32311	LMC0518-6820I	52657.914	0.487	17.19	0.03	16.77	0.03	16.64	0.09	17.85
76			LMC0514-6820G	52660.786	0.852	17.51	0.05	17.14	0.07	17.05	0.16	18.09
100	WVir	0.87105	LMC0522-7020F	53355.891	0.554	16.31	0.02	16.01	0.02	16.01	0.08	16.83
100			LMC0522-7020E	52700.891	0.411	16.13	0.02	15.79	0.02	15.91	0.06	16.71
105	BLHer	0.17298	LMC0522-7020E	52700.891	0.040	17.05	0.03	16.84	0.03	16.74	0.14	17.32
105			LMC0522-7020H	52701.758	0.622	17.63	0.07	17.13	0.07	16.92	0.21	17.93
118	WVir	1.10376	LMC0525-6800B	52673.837	0.240	15.44	0.02	15.00	0.02	14.90	0.03	16.30
118			LMC0525-6820H	52683.781	0.023	15.12	0.03	14.74	0.02	14.58	0.03	15.81
122	BLHer	0.18715	LMC0525-6840H	52683.954	0.007	17.46	0.04	17.14	0.04	17.10	0.22	18.05
122			LMC0525-6820B	52675.910	0.779	17.73	0.04	17.48	0.08	17.14	0.18	18.33
138	BLHer	0.14414	LMC0529-6840A	52684.777	0.524	17.29	0.10	17.43	0.10	16.52	0.13	18.23
138			LMC0529-6900G	52364.819	0.931	17.11	0.08	17.20	0.07	16.99	0.14	17.92
143	WVir	1.16347	LMC0529-6920G	52363.769	0.569	15.57	0.02	15.27	0.02	15.17	0.04	16.21
143			LMC0533-6920I	53331.899	0.014	14.86	0.03	14.52	0.02	14.44	0.02	15.47
146	WVir	1.00344	LMC0533-6840C	52687.758	0.228	15.63	0.02	15.25	0.02	15.12	0.03	16.39
146			LMC0533-6900I	52286.935	0.463	15.88	0.01	15.51	0.02	15.35	0.03	16.50
148	BLHer	0.42679	LMC0533-6920C	52969.042	0.572	17.13	0.02	16.85	0.02	16.66	0.07	17.73
148			LMC0533-6940I	52226.973	0.824	16.84	0.02	16.67	0.04	16.57	0.10	17.33

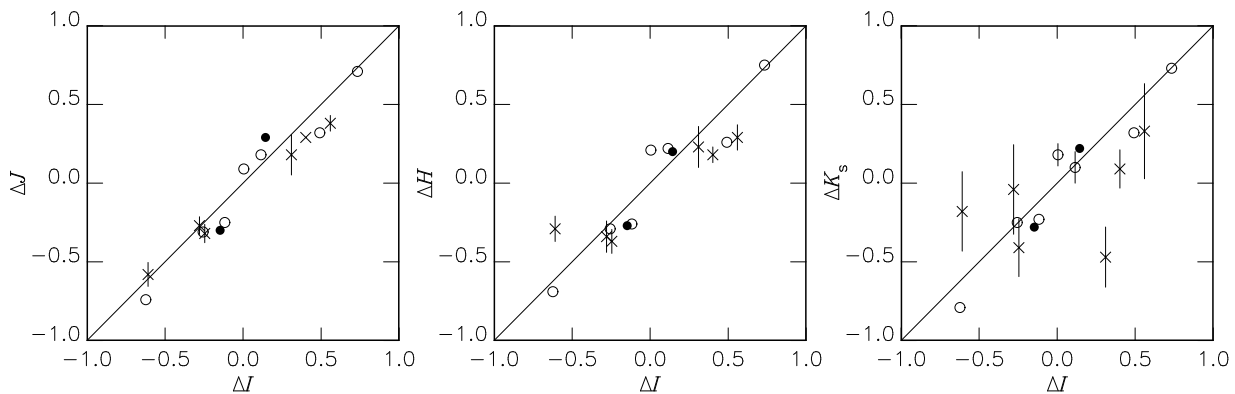


**Figure 1.** Differences of  $JHK_s$  magnitudes at two epochs of the IRSF observations are plotted against those of  $I$ -band magnitudes estimated from the OGLE light curves. Crosses indicate BLs, open circles WVs, and filled circles RVs. The error bars are omitted when their sizes are smaller than the symbols.

The slopes and (effective) zero-points do not differ significantly between the solutions for BL and WV, so that we give solutions for BL+WV stars:

$$W_5 = I - 1.55(V - I) = -2.521(\pm 0.022)(\log P - 1.2) + 14.339(\pm 0.015), (\sigma = 0.105), \quad (5)$$

and

$$W_6 = I - 1.45(V - I) = -2.486(\pm 0.022)(\log P - 1.2) + 14.440(\pm 0.15), (\sigma = 0.106). \quad (6)$$

These relations are narrow ( $\sigma \sim 0.1$ ) as expected from fig. 1 of S08.

Use of the PL( $W$ ) relation brings stars that lie below the bulk

**Table 2.** The first ten lines of the catalogue of S08 sources with IRSF counterparts. This is a sample of the full version, which will be available in the online version of this journal. Modified Julian Dates (MJD), pulsation phase of the observations,  $JHK_s$  magnitudes, and their errors are listed for each IRSF measurement as well as the OGLE-IDs, types, and periods. Shifts for the phase corrections obtained from the  $I$ -band light curves are also listed if available. Nine S08 sources are absent because their IRSF counterparts were not found, and 15 S08 sources are listed twice because they are identified with two counterparts from neighbouring fields of the IRSF survey.

OGLE-ID	Type	$\log P$	IRSF-Field		IRSF counterpart							$\delta_\phi$
			IRSF-Field	MJD(obs)	Phase	$J$	$E_J$	$H$	$E_H$	$K_s$	$E_K$	
4	BLHer	0.28240	LMC0446-6800C	52645.086	0.121	16.64	0.04	16.33	0.06	16.27	0.11	0.203
5	RVTau	1.52095	LMC0447-7000G	53037.995	0.161	13.82	0.02	13.41	0.02	13.28	0.03	0.201
6	BLHer	0.03660	LMC0450-6720B	53031.900	0.273	17.63	0.04	17.43	0.07	17.32	0.22	0.047
7	BLHer	0.09435	LMC0452-6920F	53044.963	0.224	17.50	0.04	17.25	0.06	–	–	–0.005
8	BLHer	0.24207	LMC0451-7000E	53308.910	0.293	17.25	0.02	17.34	0.06	17.31	0.17	0.130
9	BLHer	0.24584	LMC0454-6700C	53365.791	0.222	17.21	0.04	16.82	0.06	16.92	0.19	0.069
10	BLHer	0.17695	LMC0456-6840I	53062.869	0.681	17.71	0.04	17.35	0.07	17.23	0.25	–0.281
10	BLHer	0.17695	LMC0452-6840G	53049.895	0.049	17.33	0.03	17.06	0.04	16.90	0.17	0.278
11	RVTau	1.59391	LMC0453-6740G	52683.765	0.578	13.71	0.03	13.32	0.02	13.25	0.02	–
11	RVTau	1.59391	LMC0454-6720A	53017.960	0.091	13.42	0.01	13.12	0.01	13.03	0.02	–

of the Cepheids in the  $\log P$ - $V$  (and  $I$ ) diagrams and are redder than the bulk of the Cepheids PL into agreement with the others as expected for reddening-free relations. In addition we can expect that, as with classical Cepheids, Cepheids occupy an instability strip of finite width in temperature (i.e. colour). Thus a PL relation has a finite scatter and a colour term is needed to reduce this. In the case of the classical Cepheids the coefficient of the required colour term is about 1.45 (Udalski et al. 1999, van Leeuwen et al. 2007) so that  $W$  corrects in that case for both reddening and strip width.

As a first approximation we might expect the same value of  $R$  to apply in the case of the Cepheids. One can test this by looking at the residual from the  $PL(W)$  relation of the bluest stars, since it seems unreasonable to assume that the bulk of the BL stars which scatter around  $(V - I) \sim 0.7$ , are heavily reddened by interstellar extinction. There are eight BL bluer than  $(V - I) = 0.5$  which were not discarded for any of the reasons given above (stars 6, 20, 41, 71, 89, 102, 136, and 145). Their residuals from the above equation for  $W_2$  are 0.000, +0.084, –0.029, –0.145, +0.100, –0.081, +0.305, and –0.066, respectively, giving a mean of  $+0.021 \pm 0.050$  or  $-0.020 \pm 0.033$  if No. 136 is omitted. The residual for 136 is rather large and this is the bluest star in the sample. It seems possible that this might be a blend or a binary like some of the rejected stars, but this is not certain.

Taking the above results together with the colour-magnitude diagram of S08 (their fig. 2) strongly suggests that the BL stars occupy an instability strip with a width of  $\sim 0.4$  mag in  $V - I$ . The exact limits to the strip are not clearly defined. However it is important for the zero-point calibration discussed in section 4 that for an intrinsic width of this order the  $PL(W)$  relation remains narrow, indicating that in this case (as for classical Cepheid) the relation corrects well for both reddening and intrinsic colour variation.

Fig. 2 of S08 also suggests that, if the pW stars are omitted, most of the WVs occupy a narrower instability strip than the BLs, though it is uncertain whether or not the colours of some of the redder WVs are due to interstellar reddening or are intrinsic.

### 3.2 Infrared PL relations

Fig. 2 plots the phase-corrected  $JHK_s$  magnitudes against  $\log P$  for the LMC Cepheids. Note that only a few of the RVs have phase corrections applied. In the present section we give infrared PL relations for the BL and WV stars using the phase-corrected data. It

is evident from Fig. 2 that the RV stars do not continue the linear PL relations to longer periods. They are discussed in section 5.2.

Least-square solutions yield the following relations. For BL stars:

$$J_1 = -2.164(\pm 0.240)(\log P - 0.3) + 17.131(\pm 0.038),$$

$$(\sigma = 0.25, 55 \text{ stars}) \quad (7)$$

$$H_1 = -2.259(\pm 0.248)(\log P - 0.3) + 16.857(\pm 0.039),$$

$$(\sigma = 0.26, 54 \text{ stars}) \quad (8)$$

$$K_{s,1} = -1.992(\pm 0.278)(\log P - 0.3) + 16.733(\pm 0.040),$$

$$(\sigma = 0.26, 47 \text{ stars}). \quad (9)$$

For WV stars we find:

$$J_2 = -2.337(\pm 0.114)(\log P - 1.2) + 15.165(\pm 0.030),$$

$$(\sigma = 0.18, 82 \text{ stars}) \quad (10)$$

$$H_2 = -2.406(\pm 0.100)(\log P - 1.2) + 14.756(\pm 0.027),$$

$$(\sigma = 0.16, 82 \text{ stars}) \quad (11)$$

$$K_{s,2} = -2.503(\pm 0.109)(\log P - 1.2) + 14.638(\pm 0.029),$$

$$(\sigma = 0.17, 82 \text{ stars}) \quad (12)$$

The greater scatter for the BL stars compared with the WVs is at least partly due to the poorer photometry for the fainter (BL) stars, especially at the longer wavelengths. Given the uncertainties in the slopes, there is no evidence for difference between the BL and WV stars and the following are joint solutions:

$$J_3 = -2.163(\pm 0.044)(\log P - 1.2) + 15.194(\pm 0.029),$$

$$(\sigma = 0.21, 137 \text{ stars}) \quad (13)$$

$$H_3 = -2.316(\pm 0.043)(\log P - 1.2) + 14.772(\pm 0.028),$$

$$(\sigma = 0.20, 136 \text{ stars}) \quad (14)$$

$$K_{s,3} = -2.278(\pm 0.047)(\log P - 1.2) + 14.679(\pm 0.029),$$

$$(\sigma = 0.21, 129 \text{ stars}) \quad (15)$$

The slopes do not differ significantly from those found by M06 for Cepheids in globular clusters except possibly at  $K_s$  where, for

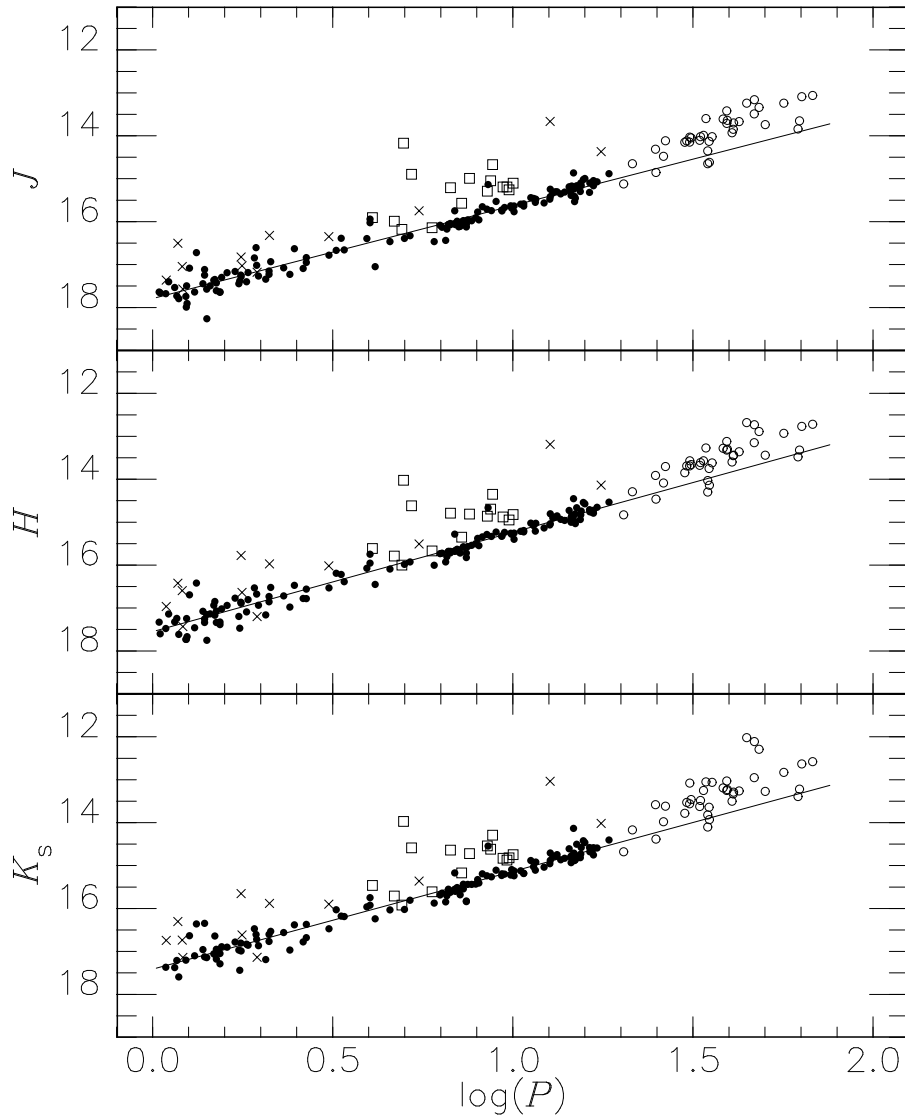


**Figure 2.** Period-magnitude relation of Cepheids in the LMC. The phase-corrected  $JHK_s$  magnitudes are plotted against periods. Filled circles indicate BL+WV used to solve the PL relations while crosses indicate those excluded, open squares pW, and open circles RV.

instance, the slope in eq. (15) is shallower by  $1.9\sigma$  compared with the cluster value. The LMC result is sensitive to whether we reject or retain some of the fainter BL stars. In the shortest period range the detection limit of the IRSF survey can introduce a bias in the PL diagram. In fact, all the stars with the IRSF  $K_s$  missing are BL stars with  $P$  shorter than 1.5 d. The slope gets steeper and agrees with the case of WV (eq. 12) if we use only those with  $P > 1.5$  d. Since the difference is in any case only of marginal significance, we have chosen to ignore it. Then, adopting the cluster slopes we obtain the following relations for the combined BL and WV set:

$$J_4 = -2.230(\pm 0.05)(\log P - 1.2) + 15.160(\pm 0.018),$$

$$(\sigma = 0.21) \quad (16)$$

$$H_4 = -2.340(\pm 0.05)(\log P - 1.2) + 14.760(\pm 0.017),$$

$$(\sigma = 0.20) \quad (17)$$

$$K_{s,4} = -2.410(\pm 0.05)(\log P - 1.2) + 14.617(\pm 0.015),$$

$$(\sigma = 0.21) \quad (18)$$

where the uncertainties in the slopes are those given by M06.

Solutions have also been made using the LMC  $JHK_s$  data uncorrected for phase. In the case of the WV stars the scatters ( $\sigma$ ) about equations analogous to (10), (11), and (12) are 0.26, 0.23, and 0.24 mag, respectively. This may be compared with the figures for the phase-corrected data; 0.18, 0.16, and 0.17 mag. Thus a significant improvement is found using the phase-corrected data and the scatter becomes comparable with that found by M06 for Cepheid in globular clusters (0.16, 0.15, and 0.14) even though the LMC results depend on a single observation per star and no allowance is made for possible differential reddening. A similar test in the case of the BL stars shows little decrease in the scatter when the phase-corrected rather than uncorrected data are used. This is probably due to the poorer quality of the photometry for these fainter stars as already noted.

**Table 3.** Estimates of the distance modulus of the LMC ( $\mu_{\text{LMC}}$ ) based on pulsation parallaxes of V553 Cen and SW Tau combined with the PL relations in this paper.

Eq.	$\mu_{\text{LMC}}$	Note
(1)	18.45	$W_1 (R = 1.55)$
(2)	18.45	$W_2 (R = 1.45)$
(7)	18.47	$J_1$
(8)	18.42	$H_1$
(9)	18.41	$K_{s,1}$
(7)–(9)	18.44	mean ( $J_1, H_1, K_{s,1}$ )
(16)	18.51	$J_4$
(17)	18.44	$H_4$
(18)	18.48	$K_{s,4}$
(16)–(18)	18.48	mean ( $J_4, H_4, K_{s,4}$ )

## 4 PL CALIBRATION AND APPLICATIONS

### 4.1 The LMC

The various PL relations discussed above can be calibrated using the two Galactic BL stars with pulsation parallaxes V553 Cen ( $\log P = 0.314$ ) and SW Tau ( $\log P = 0.200$ ) (see F08). The intrinsic colours of these stars are  $(V - I)_0 = 0.70$  and  $0.36$ . This corresponds to  $0.80$  and  $0.46$  if we redden them by an amount expected in the LMC, where we adopt as a typical mean reddening,  $E_{B-V} = 0.074$  (see Caldwell & Coulson 1985). Thus these two stars span almost the whole range suggested above for the width of the BL instability strip.

Using the data of tables 4 and 5 of F08, we can calibrate the zero-points of the various PL relations and hence estimate the modulus of the LMC ( $\mu_{\text{LMC}}$ ). In doing this the  $JHK$  data of F08 were converted from the SAAO system into that of the IRSF using the transformations from SAAO to 2MASS (Carpenter 2001 and web site updates) and those from 2MASS to IRSF using the relations of Kato et al (2007). We obtain  $\mu_{\text{LMC}}$  estimates between 18.41 and 18.51 based on different PL relations obtained above as listed in Table 3.

The uncertainties to be associated with these values are of interest. The uncertainties estimated for the distance moduli of V553 Cen and SW Tau are each  $0.08$  (F08). This thus contributes  $0.06$  to the uncertainties in the above mean results. In fact the  $W$  zero-points derived from the two stars differ by  $0.2$  mag, i.e. an uncertainty in the mean of  $0.10$ . On the other hand the two stars give mean zero-points for the  $JHK_s$  relations with formal uncertainties of only  $\sim 0.04$  mag. These figures of course have their own, considerable, uncertainty. However, remembering the range in intrinsic  $(V - I)$  of the two stars, they suggest very narrow  $JHK_s$  PL relations. The scatter quoted above for the infrared PL relations must be largely due to observational effects, especially in the case of the BL star.

Taken together these results suggest  $\mu_{\text{LMC}}$  of  $18.46$  mag. They also suggest an uncertainty of less than  $0.10$  mag but to be reasonably conservative we adopt this as the standard error. No account is taken in this of any possible metallicity effects. These values agree well with those derived from classical Cepheids with trigonometrical parallaxes by van Leeuwen et al. (2007) and Benedict et al. (2007). These authors found  $18.52 \pm 0.03$  from a PL( $W$ ) relation and  $18.47 \pm 0.03$  from a PL( $K_s$ ) relation again without metallicity

corrections. In the case of the PL( $W$ ) relation this gave a modulus of  $18.39 \pm 0.05$  when a recent metallicity correction (Macri et al. 2006) was applied, though this correction has been questioned (Bono et al. 2008). These results suggest that any metallicity correction to the PL( $W$ ) result for Cepheids will be small. M06 found no evidence for a metallicity correction to the  $JHK_s$  PL relations based on globular clusters. Current theoretical work (Bono, Caputo, & Santolamazza, 1997; Di Criscienzo et al. 2007) suggests that the evolutionary and pulsational properties of Cepheids are only minimally affected by metallicity.

### 4.2 The distance to the Galactic centre

The distance to the Galactic centre ( $R_0$ ) based on the Cepheids in the Galactic bulge was discussed in F08 on the basis of the parallaxes of V553 Cen and SW Tau and the  $K$ -band observations of Groenewegen, Udalski & Bono (2008). A value of  $R_0 = 7.64 \pm 0.21$  kpc was obtained. The quoted standard error does not take into account any systematic error in the corrections for reddening adopted by Groenewegen et al. (2008). These corrections are substantial, ranging from  $0.16$  to  $0.69$  mag at  $K$ , and this may be a significant uncertainty in the method. It is possible in principle to use reddening-free relations. Groenewegen et al. illustrated this using the colour,  $(I - K)$ . However, in view of the high reddening of the stars used, the result is very sensitive to the coefficient used in the reddening-free relation (equivalent to  $R$  in section 3.1). Infrared colours (e.g.  $J - K$  or  $H - K$ ) may be more successful when the relevant data are available.

### 4.3 NGC 6441

NGC 6441 is an outstanding example of a 'second-parameter' globular cluster. It is of relatively high metal ( $[\text{Fe}/\text{H}] = -0.53$ ) but has an extended horizontal branch and RR Lyrae variables. The RR Lyraes seem to be evolved and brighter than expected for their metallicity (Pritzl et al. 2003, hereafter P03). The cluster also contains Cepheid for which P03 give  $VI$  photometry. The reddening is large,  $E_{B-V} = 0.51$  according to P03, and possibly uncertain. This is therefore a useful cluster to study with a reddening-free parameter. A solution of the data for the seven Cepheids, taking  $W = I - 1.45(V - I)$  is,

$$W = -2.549(\pm 0.040) \log P + 14.439(\pm 0.044) \quad (19)$$

The slope is not significantly different from that found for the LMC Cepheids. Calibrating this relation using the data on V553 Cen and SW Tau leads to a cluster modulus of  $15.46 \pm 0.11$  mag. This is very close to the value ( $15.48$ ) adopted by P03 on the assumptions that the RR Lyraes in this metal-rich cluster have absolute magnitudes similar to those with  $[\text{Fe}/\text{H}] \sim -2.0$  and that  $E_{B-V} = 0.51$ . Note however that the visual absolute magnitudes of the RR Lyraes depend critically on the reddening adopted.

M06 list mean  $JHK_s$  values for two Cepheids in NGC 6441. However one of these (V129) may be affected by blending (see section 5.1) and we omit this star. The data on the other star (V6) can be used together with the PL relations in M06 and the data on V553 Cen and SW Tau to obtain another estimate of the modulus. Adopting the same reddening as above we obtain a modulus of  $15.49 \pm 0.05$  consistent with the value just given from PL( $W$ ). This infrared modulus also depends on the adopted reddening. However this cannot be made much smaller if the intrinsic colours of the NGC 6441 Cepheids,  $(V - I)_0$ , are similar to those of the LMC Cepheids.

#### 4.4 $\kappa$ Pavonis

$\kappa$  Pav ( $\log P = 0.959$ ) has long been thought of as probably the nearest CephII and hence a prime candidate for fixing the distance scale for these objects. However, the results given in F08 were puzzling. An apparently good pulsation parallax with a small error was derived leading to a distance modulus of  $6.55 \pm 0.07$ . The revised Hipparcos parallax led to a modulus of  $5.93 \pm 0.26$ ; a  $2\sigma$  difference from the pulsation parallax. It was recognized in F08 that the pulsation parallax implied that the star was brighter than expected for a CephII. If we adopt a LMC modulus of 18.5, the star is 0.40 mag brighter than the LMC PL( $W$ ) relation at its period, 0.52 mag brighter than the PL( $J$ ) relation and 0.43 mag brighter than the PL( $K_s$ ) relation. If the LMC is closer than 18.5 mag, as suggested above, these differences will be increased.

Comparison of the data for  $\kappa$  Pav (table 5 of F08) with fig. 1 of S08 shows that in  $V$  and  $I$  as well as  $W$  the star lies above the normal CephII stars and in the region of the pW stars which was identified by S08. Further evidence that  $\kappa$  Pav belongs to the pW class is given by its colour. Its intrinsic colour is  $(V - I)_0 = 0.66$ , hence  $(V - I) = 0.76$  if the star is reddened by an amount comparable with the LMC stars. Comparison with the data of S08 (e.g. their fig. 2) shows that these colours are bluer than normal CephIIs of this period (WV stars) and fall in the region occupied by the pW stars.

There are two further indications that  $\kappa$  Pav belongs to the pW class. The revised Hipparcos data discussed in F08 indicate that the star probably had a close companion. This is consistent with the fact that S08 find a high proportion, and probably all, pW variables are binaries. Finally, S08 pick out pW stars based on their light curves, the rising branch being steeper than the declining one. Comparison of the light curve of  $\kappa$  Pav = HIP 093015 (ESA 1997, Vol 12) with the examples in S08 fig. 5 strongly suggests that it should be classed with the pW variables.

## 5 THE INFRARED COLOURS OF TYPE II CEPHEIDS

In this section we discuss and compare the infrared colours of CephIIs in the LMC and those in globular clusters (section 5.1 for BL and WV, and 5.2 for RV). This section is essentially descriptive and further data are required (for instance on the metallicities of the LMC stars) before detailed interpretation of the phenomena noted can be made.

Fig. 3 presents the colour-magnitude in the panel (a) and colour-colour diagrams in the panels (b), (c), and (d) for BL, WV+pW, and RV variables, respectively. Symbols are as in Fig. 2, and the uncertainties in colour are indicated by error bars if they exceed the size of the symbols. We also plot CephIIs in globular clusters (M06) in the colour-colour diagram using grey star symbols, and Galactic RV stars from Lloyd Evans (1985) in the panel (d) with triangles. The magnitudes of the latter sample were converted from the SAAO system to that of the IRSF as described in section 4.1. No reddening corrections were applied to the LMC objects and the Galactic ones, while, for the cluster variables, the dereddened colours have been adjusted for the mean LMC reddening ( $E_{B-V} = 0.074$  mag assumed as in section 4.1). The curve in the two-colour plots is the location of normal giants (G0III-K5III) from Bessell & Brett (1988) whose colours are also transformed into the IRSF/SIRIUS system after adding LMC reddening.

The infrared colour/ $\log P$  relations are plotted in Fig 4. Symbols are the same as in Fig. 3 but the Galactic RVs are not included.

As in the colour-colour plots, the dereddened magnitudes of the globular-cluster objects have been reddened by an amount corresponding to the adopted LMC reddening, so that the two samples are directly comparable. Discussions on these diagrams are given below.

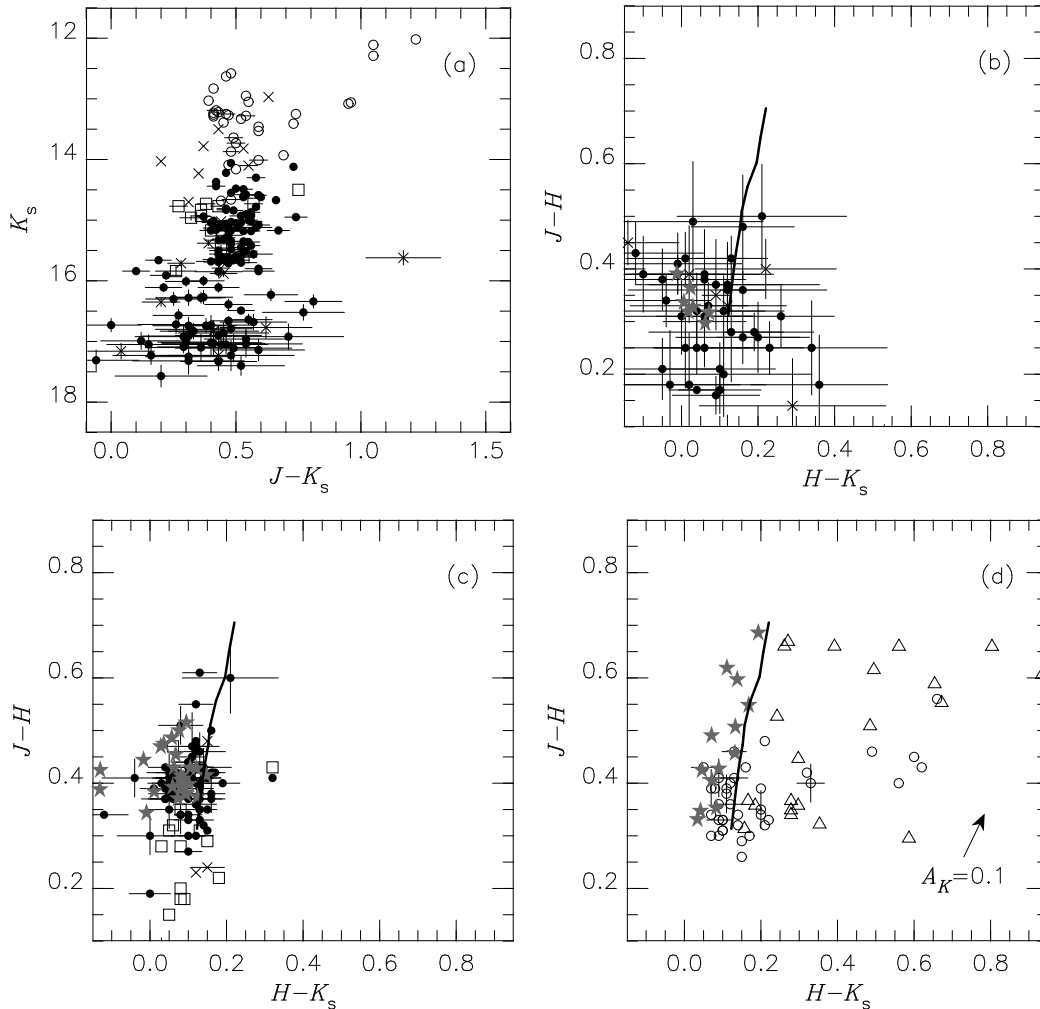
### 5.1 BL Her and W Vir variables

Fig 3 shows that in the colour-colour plots the cluster stars are systematically bluer in  $H - K_s$  than the local field stars (the thick line). This can be explained, at least in a qualitative sense, by metallicity difference; the locus by Bessell & Brett (1988) is based on local giants probably of the solar abundance, while the cluster stars are metal-poor. If we consider giants with different metallicities but with the same surface temperature (in a range of 4000–5500 K), a metal-poor giant is expected to be bluer than a giant with the solar abundance in  $H - K_s$  but has almost the same colour in  $J - H$  (Westera et al. 2002).

In the case of the BL variables the photometric uncertainties are rather large for the LMC objects, especially in  $K_s$ , and it is difficult to discuss the distribution of colours. On the other hand, most of the WV stars in the LMC form a relatively dense grouping in the panel (c) of Fig. 3, and many of the globular-cluster stars lie in the same region. There is a conspicuous 'line' of cluster variables to the upper left of the main grouping. We have not found any strong differences between these stars and other cluster WV stars. Two cluster variables are on the extreme left of the Fig. 3 (c). One of these stars is the variable in the cluster Terzan 1. The reddening of this cluster is high (M06 used  $E_{B-V} = 2.28$ ) and probably rather uncertain and this makes its true position in Fig. 3 (c) uncertain. The other star is V129 in NGC 6441. This star lies in a rather crowded region of the cluster and the colours may be affected by blending.

In Fig. 5, we plot period histograms for CephIIs in the LMC (top) and globular clusters (bottom). In the LMC histogram the pW stars are omitted. The hatched areas indicate the period distribution of the objects whose near-infrared magnitudes are discussed in this study. Several known CephIIs in globular clusters, which were not observed by M06 are collected from the catalogue in Pritzl et al. (2003) and added as the white area in the lower panel. A significant number of short-period BLs were not included in M06 because of their faintness. The previous surveys of variables with period longer than 1 d are not complete for globular clusters.

Fig. 5 shows a minimum in both the LMC and cluster distributions near 4 d. This is qualitatively consistent with the division between the BL and WV stars as summarized in section 1. However there are clear differences between the two distributions at longer periods. In the range  $0.6 < \log P < 1.0$ , there is an excess of variables in the LMC compared with the clusters. The period distribution of the Galactic field WVs discussed by Wallerstein & Cox (1984) seems similar to that of the LMC field. However, a caution is required in this comparison since various selection biases will affect the Galactic field sample including the fact that it presumably includes Galactic field pW stars such as  $\kappa$  Pav. In the LMC the pW stars are most frequent in the range  $0.6 < \log P < 1.0$ . It is notable that a relatively sharp peak at  $\log P \sim 1.2$  exists in both panels of Fig. 5. Whilst the deficiency of globular variables in the range  $0.6 < \log P < 1.0$  is in broad qualitative agreement with Gingold's models, the excess of variables in this period range in the LMC field (and probably also the Galactic field) is not so easily understood (see Gingold 1985, especially section 9). However the referee has pointed out to us that the position of the



**Figure 3.** Colour-magnitude and colour-colour diagrams for Cepheids. The panel (a) includes all the types of the LMC Cepheids, while the panels (b), (c), and (d) are for BL, WV+pW, and RV stars, respectively. Symbols are the same as in Fig. 2 for the LMC objects, while those in globular clusters are indicated by star symbols. The triangles, in the panel (d), are for Galactic field RV stars from Lloyd Evans (1985). Error bars are indicated for the LMC Cepheids only if an uncertainty significantly exceeds the size of the symbols. The thick curves are the loci of local giants (see text for details).

loops found by Gingold are not supported by modern models (e.g. Pietrinferri et al. 2006). A closer comparison with theory is clearly desirable but outside the scope of this paper. The gap seen in the top panel of Fig. 5 at 20 d, separating the LMC WV and RV stars is not present in the cluster sample. This will be discussed in section 5.2.

In Fig. 4, WVs in the LMC and globular-cluster groups have about the same colours at a given period. In the case of the clusters, however, there is a curious tendency in the range  $1.0 < \log P < 1.3$  for  $(J - H)$  and  $(J - K_s)$  to become bluer with increasing period. This amounts to a change in  $J - H$  from  $\sim 0.45$  at  $\log P = 1.10$  to  $\sim 0.35$  at  $\log P = 1.25$ . Those relatively red objects at around  $\log P = 1.1$  belong to the outstanding 'line' mentioned above. Whether this feature, which is not shared by the LMC stars, is significant, and if so what it implies, remains to be investigated.

## 5.2 RV Tauri variables

The classical definition of an RV star is the alternating depth of their minima. However the distinction between them and the longer-period WV stars is not very clear. S08 adopt a division at a period

(single cycle) of 20 d. The RVs are a heterogeneous group as has long been realized (Preston et al. 1963) and at least some are binaries. It is clear from the LMC period-magnitude diagrams (Fig. 2, and fig. 1 of S08) that any PL relation has a considerable scatter though they continue the general increase of brightness with increasing period shown by the shorter-period Cepheids. In the case of the  $JHK_s$  data the plots use instantaneous magnitudes for most of the stars, since phase correction is difficult for these stars; their periods and light curves tending in many cases to be rather unstable.

It is particularly notable that the RVs as defined by S08 do not lie on a linear extension of the PL relations defined by shorter-period Cepheids ( $JHK_s$  and  $W$  PL relations). These LMC RVs all have  $\log P$  in the range 1.3 to 1.8. As can be seen from fig. 3 of M06 Cepheids in globular clusters in this period range are co-linear with the shorter-period stars in  $JHK_s$  PL diagrams.

Further evidence for differences between the RVs in clusters and those in the LMC is found in the period-colour relation (Fig. 4). At the shorter periods among the RVs,  $\log P \leq 1.5$ , the cluster and LMC stars tend to lie together. They remain together for  $\log P > 1.5$  in the case of the  $H - K_s$  colours except for the LMC objects with  $K_s$ -band excess, see below, but the situation is different in



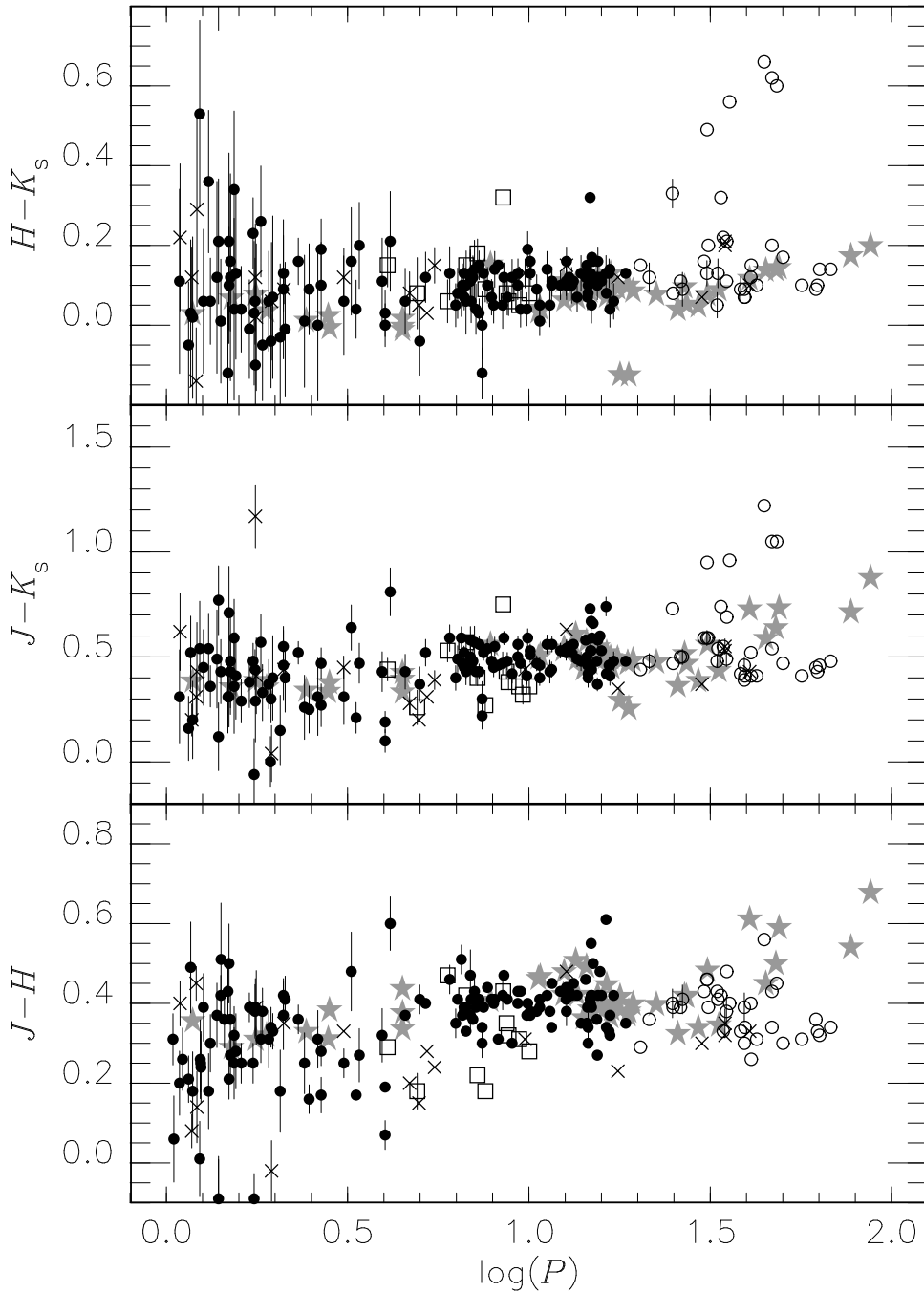


**Figure 4.** Period-colour relation. Symbols are the same as in Fig. 3. Error bars are indicated for the LMC CepHIs only if an uncertainty significantly exceeds the size of the symbols.

$J - K_s$  and  $J - H$ . The cluster RVs are redder in  $J - H$ , while they tend to occupy a region between the bluer LMC stars and those with an infrared excess in the case of  $J - K_s$ .

The LMC RVs with the excesses include the three brightest stars at  $K_s$  (32, 67, 174). They are also the three reddest stars in Fig. 3, and stand out clearly in the  $\log P - K_s$  diagram (Fig. 2). The next two stars which are reddest in  $J - K_s$  (both with mild infrared excesses) are numbers 91 and 180. Welch (1987) already noted numbers 67 (HV 915) and 91 (HV 2444) as having infrared excesses. No. 119 (HV 5829) which has a comparable excess to

these two stars in Welch’s work has the next reddest  $H - K_s$  in the IRSF data to the five stars just mentioned.

In the colour-colour diagram (Fig. 3d), the LMC stars with significant  $K_s$  excesses lie at  $(H - K_s) \sim 0.6$ . Most of the others lie relatively close to the intrinsic line, though some may have a very mild excess at  $K_s$ . Galactic RV stars from Lloyd Evans (1985), triangles in Fig. 3, show a rather dispersed distribution; their  $J - H$  colours range from 0.1 to 0.7 mag. No reddening correction was applied to their colours, and some of the stars may be affected significantly. However, this is not likely to change the overall impression left by the plot. Whilst there may be some overlap between

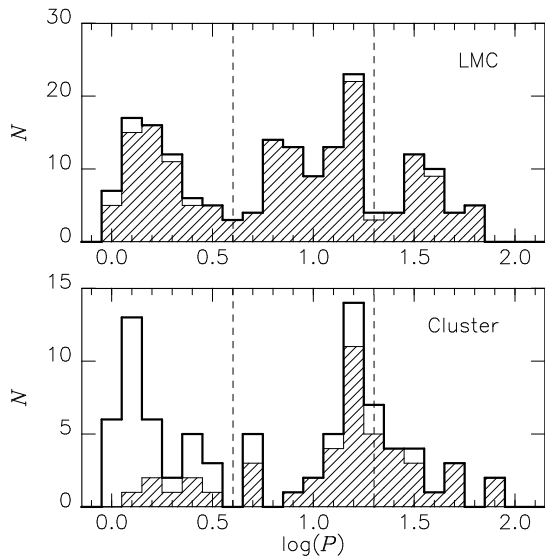


**Figure 5.** Histograms of periods for the Cepheids: the top panel is for the LMC objects from the S08 catalogue and the lower panel is for those in globular clusters from a combined catalogue of M06 and P03 (see text for details). The hatched areas indicate the period distribution of the objects whose near-infrared magnitudes are discussed in this study. Vertical lines indicate period divisions adopted by S08.

the three populations (clusters, the LMC, and the Galaxy), in general they form distinctly different groupings. Their differences have been also noted by Russell (1998), Zsoldos (1998), and M06.

It should be realized that in contrast to the LMC and globular-cluster samples we do not know the absolute magnitudes of the Galactic sample; or indeed, whether they all are in the same evolutionary phase. So far as the cluster RVs are concerned, we examined the locations of those with periods greater than 40 d, that is the most luminous stars of the samples, in  $K_s-(J-K_s)$  diagrams (Matsunaga 2007). They all lie well down the giant branch except possibly for NGC 1904 V8 which is near the top. Thus these longer-period stars in clusters might well be on loops from the AGB like the, shorter-period, WV stars. The histograms of Fig. 5 would be consistent with the view that for  $P > 20$  d the cluster variables are simply the long-period tail of the distribution of WVs whereas in the LMC there is a distinct population at these periods.

Low-resolution spectra covering the range  $\sim 3800$  to  $7800 \text{ \AA}$  of all 36 of the OGLE-III RV stars were obtained in the period 2009 January 16–20, except for numbers 32, 58, and 162. The observations were made with the Cassegrain spectrograph on the 1.9-m reflector at SAAO, Sutherland. No. 15 had strong  $C_2$  bands and is the only one of the sample to show  $C_2$ . Lloyd Evans & Pollard (2004) examined a sample of LMC RV stars, including those discovered in the MACHO survey and found this star (Macho 47.2496.8) to be the only one in their sample with  $C_2$  bands (see also Pollard & Lloyd Evans 2000). However, this star is not particularly outstanding in any of Fig. 3 and 4. Note that there must be some overlap between the two samples although Lloyd Evans & Pollard (2004) do not list the stars they studied. Our spectra show the presence of TiO in numbers 45, 75, 104, 125, 135, 149, 169 and also probably in 25, 51, 112. Since the TiO bands are known to vary in strength with phase, it may well be present in other stars of the sample at other times. Lloyd Evans & Pollard (2004) previously noted weak TiO in 169 = HV 12631. The most sensitive indicator of the

presence of TiO in our spectra is the  $\alpha$  system sequence beginning near  $6159 \text{ \AA}$ .

## 6 CONCLUSIONS

We obtained PL relations in phase-corrected  $JHK_s$  magnitudes for the combined set of BL and WV stars in the LMC. They have slopes consistent with those found previously (M06) in globular clusters. For the WV stars, the scatter about the PL relations is significantly reduced using the phase-corrected data. The longer-period variables (RVs) show a significant scatter in the infrared and reddening-free ( $VI$ ) PL relations and as a group they are not colinear with the shorter-period stars. This contrasts with the situation for Cepheids in globular clusters. It remains to be determined whether those RV stars which do lie near an extrapolation of the PLs from the shorter-period can be distinguished from the others in some way, e.g. from radial velocity or spectral features. Differences in infrared period-colour, colour-colour and period-frequency diagrams are found for the WV stars in the LMC and in Galactic globular clusters. In the case of Cepheid stars with  $P > 20$  d (RV stars) there are marked differences between the available samples of the LMC, Galactic globular cluster and the Galactic field and little evidence that the cluster stars are post-AGB objects. A new class of Cepheids (pW) was identified by S08, and we suggest that the bright Galactic star  $\kappa$  Pav belongs in this class. Such stars have not, so far, been identified in globular clusters and may thus be younger objects.

When the PL relations are calibrated using the pulsation parallaxes of V553 Cen and SW Tau we find a distance modulus for the LMC of  $18.46 \pm 0.10$  mag without any metallicity correction, consistent with other recent determinations. Applying our calibration to the Cepheid stars in the second-parameter globular cluster NGC 6441 leads to a modulus of  $15.46 \pm 0.11$  mag which confirms the view that the RR Lyraes in this cluster are overluminous for their metallicity.

## ACKNOWLEDGMENTS

We thank the referee G. Bono for his comments and especially for drawing our attention to some theoretical papers.

## REFERENCES

- Benedict G. F. et al., 2007, *AJ*, 133, 1810
- Bessell M. S., Brett J. M., 1988, *PASP*, 100, 1134
- Bono G., Caputo F., Santolamazza P., 1997, *A&A*, 317, 171
- Bono G., Caputo F., Fiorentino G., Marconi M., Musella I., 2008, *ApJ*, 684, 102
- Caldwell J. A. R., Coulson I. M., 1985, *MNRAS*, 212, 879
- Cardelli J. A., Clayton G. C., Mathis J. S., 1989, *ApJ*, 345, 245
- Carpenter J. M., 2001, *AJ*, 121, 2851
- Di Criscienzo M., Caputo F., Marconi M., Cassisi S., 2007, *A&A*, 471, 893
- ESA, 1997, The Hipparcos catalogue ESA SP-1200
- Feast M. W., Laney C. D., Kinman T. D., van Leeuwen F., Whitlock P. A., 2008, *MNRAS*, 386, 2115 (F08)
- Freedman W. L., et al., 2001, *ApJ*, 553, 47
- Gingold R. A., 1976, *ApJ*, 204, 116
- Gingold R. A., 1985, *Mem.Soc.Astron.Ital.*, 56, 169
- Groenewegen M.A.T., Udalski A., Bono G., 2008, *A&A*, 481, 441

- Kato D. et al., 2007, PASJ, 59, 615  
Lloyd Evans T., 1985, MNRAS, 217, 493  
Lloyd Evans T., Pollard K. R., 2004, ASPC, 310, 344  
Macri L. M., Stanek K. Z., Bersier D., Greenhill L. J., Reid M. J.,  
2006, ApJ, 652, 1133  
Matsunaga N., 2007, PhD thesis, The University of Tokyo  
Matsunaga N. et al., 2006, MNRAS, 370, 1979 (M06)  
Pietrinferri A., Cassisi S., Salaris M., Castelli F., 2006, ApJ, 642,  
797  
Pollard K. R., Lloyd Evans T., 2000, AJ, 120, 3098  
Preston G. W., Krzeminski W., Smak J., Williams J. A., 1963,  
ApJ, 137, 401  
Pritzl B. J., Smith H. A., Stetson P. B., Catelan M., Sweigart A. V.,  
Layden A. C., Rich R. M., 2003, AJ, 126, 1381 (P03)  
Russell S. C., 1998, PASA, 15, 189  
Schlegel D. J., Finkbeiner D. P., Davis M., 1998, ApJ, 500, 525  
Skrutskie M. F. et al. 2006, AJ, 131, 1163  
Soszyński I. et al., 2008, Acta Astron., 58, 293 (S08)  
Udalski A., Szymański M., Kubiak M., Pietrzyński G., Soszyński  
I., Woźniak P., Zebrun K., 1999, Acta Astron., 49, 201  
van Leeuwen F., Feast M. W., Whitelock P. A., Laney C. D., 2007,  
MNRAS, 379, 723  
Wallerstein G., Cox A. N., 1984, PASP, 96, 677  
Welch D. L., 1987, ApJ, 317, 672  
Westera P., Lejeune T., Buser R., Cuisinier F., Bruzual G., 2002,  
A&A, 381, 524  
Zsoldos E., 1998, Acta Astron., 48, 775

**ONLINE MATERIAL**

What follows is the full version of Table 2. The presented data will be available in the online version of MNRAS.

**Table 4.** A catalogue of the S08 sources with IRSF counterparts (the full version of Table 2). Modified Julian Dates (MJD), pulsation phase of the observations,  $JHK_s$  magnitudes, and their errors are listed for each IRSF measurement as well as the OGLE-IDs, types, and periods. Shifts for the phase corrections obtained from the  $I$ -band light curves are also listed if available. Nine S08 sources are absent because their IRSF counterparts were not found, and 15 S08 sources are listed twice because they are identified with two counterparts from neighbouring fields of the IRSF survey.

OGLE-ID	Type	log $P$	IRSF counterpart									$\delta_\phi$
			IRSF-Field	MJD(obs)	Phase	$J$	$E_J$	$H$	$E_H$	$K_s$	$E_K$	
4	BLHer	0.28240	LMC0446-6800C	52645.086	0.121	16.64	0.04	16.33	0.06	16.27	0.11	0.203
5	RVTau	1.52095	LMC0447-7000G	53037.995	0.161	13.82	0.02	13.41	0.02	13.28	0.03	0.201
6	BLHer	0.03660	LMC0450-6720B	53031.900	0.273	17.63	0.04	17.43	0.07	17.32	0.22	0.047
7	BLHer	0.09435	LMC0452-6920F	53044.963	0.224	17.50	0.04	17.25	0.06	–	–	–0.005
8	BLHer	0.24207	LMC0451-7000E	53308.910	0.293	17.25	0.02	17.34	0.06	17.31	0.17	0.130
9	BLHer	0.24584	LMC0454-6700C	53365.791	0.222	17.21	0.04	16.82	0.06	16.92	0.19	0.069
10	BLHer	0.17695	LMC0456-6840I	53062.869	0.681	17.71	0.04	17.35	0.07	17.23	0.25	–0.281
10	BLHer	0.17695	LMC0452-6840G	53049.895	0.049	17.33	0.03	17.06	0.04	16.90	0.17	0.278
11	RVTau	1.59391	LMC0453-6740G	52683.765	0.578	13.71	0.03	13.32	0.02	13.25	0.02	–
11	RVTau	1.59391	LMC0454-6720A	53017.960	0.091	13.42	0.01	13.12	0.01	13.03	0.02	–
12	WVir	1.06374	LMC0456-6820C	53400.962	0.136	15.43	0.02	14.98	0.02	14.87	0.03	0.048
13	WVir	1.06238	LMC0455-7000G	53309.080	0.798	15.51	0.02	15.17	0.02	15.07	0.03	0.039
14	RVTau	1.79152	LMC0455-7000G	53309.080	0.552	13.84	0.01	13.48	0.01	13.39	0.02	–
15	RVTau	1.75221	LMC0457-6800I	52675.879	0.376	13.24	0.01	12.93	0.02	12.83	0.02	–
16	RVTau	1.30740	LMC0456-6900B	53019.827	0.620	15.12	0.01	14.83	0.01	14.68	0.02	–
17	WVir	1.16001	LMC0456-6820H	53053.855	0.031	14.98	0.01	14.63	0.01	14.48	0.02	0.323
18	BLHer	0.13975	LMC0459-6920B	53060.840	0.483	17.60	0.04	17.23	0.07	17.11	0.23	–0.153
19	pWVir	0.93826	LMC0500-6800C	53039.914	0.173	15.20	0.01	14.85	0.02	14.77	0.03	–
20	BLHer	0.04459	LMC0500-6740C	52604.984	0.503	17.60	0.05	17.34	0.06	–	–	–0.201
21	pWVir	0.98943	LMC0501-7120I	52935.117	0.360	15.46	0.02	15.15	0.02	15.02	0.03	–
22	WVir	1.03006	LMC0458-7040G	53497.695	0.076	15.44	0.02	15.05	0.02	15.04	0.03	0.144
22	WVir	1.03006	LMC0502-7040I	53117.759	0.623	15.75	0.02	15.34	0.02	15.29	0.03	–0.112
23	pWVir	0.71890	LMC0500-6740E	52605.016	0.366	15.01	0.02	14.73	0.02	14.70	0.02	–
24	BLHer	0.09575	LMC0503-6940C	53414.925	0.874	17.78	0.04	17.54	0.08	–	–	0.127
25	RVTau	1.83229	LMC0503-6840I	53301.999	0.989	13.06	0.02	12.72	0.01	12.58	0.01	–
26	WVir	1.13283	LMC0504-6820F	53123.705	0.243	15.33	0.02	14.91	0.02	14.84	0.03	0.025
27	WVir	1.23385	LMC0503-6940E	53053.791	0.478	15.51	0.02	15.09	0.02	15.03	0.04	–0.438
28	pWVir	0.94373	LMC0502-7000B	53083.751	0.192	15.11	0.02	14.79	0.02	14.73	0.03	–
29	RVTau	1.49479	LMC0503-6840E	53301.952	0.393	14.05	0.02	13.66	0.01	13.46	0.02	–
30	BLHer	0.59499	LMC0504-6800B	53118.735	0.170	16.28	0.03	15.96	0.06	15.85	0.09	0.113
31	WVir	0.82646	LMC0506-7120I	52932.098	0.905	15.99	0.02	15.66	0.02	15.56	0.03	0.054
32	RVTau	1.64896	LMC0504-6720B	53344.945	0.762	13.24	0.01	12.68	0.01	12.02	0.01	–
33	pWVir	0.97288	LMC0503-6900G	53305.936	0.099	15.19	0.02	14.88	0.02	14.83	0.02	–
34	WVir	1.17351	LMC0503-6900A	53302.014	0.084	15.18	0.01	14.76	0.01	14.59	0.02	0.274
35	WVir	0.99414	LMC0503-6920D	53375.777	0.942	15.54	0.01	15.17	0.01	15.13	0.04	0.090
36	WVir	1.17262	LMC0507-6920C	52612.966	0.513	15.54	0.02	15.15	0.02	15.10	0.04	–0.343
37	WVir	0.83869	LMC0506-7120E	52921.052	0.510	16.09	0.02	15.72	0.03	15.59	0.05	–0.039
38	WVir	0.60354	LMC0503-6840A	53123.751	0.964	15.94	0.02	15.87	0.03	15.84	0.05	0.084
38	WVir	0.60354	LMC0507-6840C	53341.916	0.320	15.85	0.01	15.66	0.02	15.66	0.05	0.089
39	WVir	0.94031	LMC0504-6720G	53354.888	0.426	15.83	0.01	15.42	0.02	15.35	0.04	–0.087
40	pWVir	0.98345	LMC0506-6940C	53308.992	0.829	15.28	0.02	–	–	14.96	0.04	–
41	BLHer	0.39377	LMC0507-6920F	52613.016	0.105	16.55	0.02	16.39	0.03	16.30	0.11	0.080
42	pWVir	0.69220	LMC0507-6920I	52613.884	0.120	16.10	0.02	15.92	0.04	15.84	0.08	–
43	WVir	0.81687	LMC0506-7000H	53080.865	0.265	16.18	0.02	15.81	0.02	15.71	0.05	–0.007
44	WVir	1.12287	LMC0506-6940B	53308.980	0.384	15.49	0.02	15.04	0.01	14.93	0.02	–0.186
45	RVTau	1.80200	LMC0506-6940H	53309.089	0.315	13.09	0.02	12.77	0.01	12.63	0.01	–
46	WVir	1.16861	LMC0507-6820E	53081.785	0.371	14.85	0.01	14.44	0.01	14.12	0.02	0.013
47	WVir	0.86250	LMC0506-6940D	53309.004	0.917	15.93	0.02	15.53	0.02	15.50	0.03	0.045
48	BLHer	0.16000	LMC0507-6820A	53078.859	0.689	17.77	0.04	17.41	0.06	–	–	–0.274
49	BLHer	0.50991	LMC0510-6940I	53333.028	0.613	16.87	0.04	16.39	0.09	16.23	0.10	–0.201

Table 4. –continued.

OGLE-ID	Type	log $P$	IRSF counterpart									$\delta_\phi$
			IRSF-Field	MJD(obs)	Phase	$J$	$E_J$	$H$	$E_H$	$K_s$	$E_K$	
50	RVTau	1.54093	LMC0511-6840C	53051.855	0.304	14.35	0.02	14.03	0.01	13.82	0.02	–
50	RVTau	1.54093	LMC0511-6900I	52612.916	0.672	14.65	0.03	14.30	0.02	14.10	0.02	–
51	RVTau	1.60859	LMC0511-6900I	52612.916	0.627	13.93	0.02	13.60	0.02	13.50	0.02	–
52	pWVir	0.67098	LMC0510-7000E	53322.849	0.132	15.99	0.02	15.79	0.02	15.71	0.05	–
53	BLHer	0.01828	LMC0511-6800E	53051.893	0.747	17.98	0.04	17.67	0.05	–	–	–0.342
54	WVir	0.99674	LMC0510-7020D	53136.698	0.196	15.67	0.02	15.27	0.02	15.08	0.04	0.013
55	RVTau	1.61284	LMC0511-6800H	53060.790	0.730	13.70	0.02	13.44	0.01	13.29	0.02	–
56	WVir	0.86271	LMC0510-6940G	53333.007	0.167	15.98	0.02	15.57	0.02	15.42	0.03	0.013
57	WVir	1.22095	LMC0511-6840D	53051.872	0.704	15.29	0.02	14.96	0.02	14.83	0.03	–0.187
58	RVTau	1.33209	LMC0511-6840G	53060.769	0.606	15.14	0.02	14.78	0.02	14.66	0.03	–0.490
59	WVir	1.22365	LMC0510-7040G	53322.877	0.012	14.68	0.01	14.36	0.02	14.22	0.02	0.365
59	WVir	1.22365	LMC0514-7040I	52714.762	0.677	15.42	0.02	15.05	0.02	15.01	0.04	–0.258
60	BLHer	0.09223	LMC0514-7020I	52697.744	0.853	17.58	0.05	17.57	0.08	17.04	0.22	0.162
61	BLHer	0.07244	LMC0514-6900C	52595.083	0.780	17.77	0.04	17.59	0.09	17.57	0.18	0.023
62	WVir	0.78152	LMC0514-6940F	52593.994	0.109	16.43	0.02	15.97	0.03	15.84	0.06	0.033
63	WVir	0.84039	LMC0514-7000H	52692.884	0.233	16.08	0.02	15.67	0.02	15.61	0.05	–0.011
64	BLHer	0.32795	LMC0514-6840E	52650.823	0.603	17.13	0.03	16.72	0.05	16.73	0.16	–0.198
65	RVTau	1.54475	LMC0514-6900E	52598.969	0.170	14.13	0.03	13.75	0.02	13.64	0.02	–
66	WVir	1.11758	LMC0515-6720H	52305.855	0.288	15.45	0.02	15.03	0.02	14.93	0.04	–0.147
67	RVTau	1.68333	LMC0514-6920H	52594.975	0.629	13.34	0.01	12.89	0.01	12.29	0.02	–
68	BLHer	0.20664	LMC0514-6900E	52598.969	0.607	17.38	0.03	17.13	0.04	17.09	0.10	–0.190
70	WVir	1.18859	LMC0515-6640E	52288.779	0.645	15.31	0.01	15.04	0.02	14.94	0.03	–0.209
71	BLHer	0.06151	LMC0514-6900G	52599.001	0.169	17.39	0.03	17.18	0.05	17.23	0.15	0.144
72	WVir	1.16178	LMC0515-6700D	52338.794	0.897	15.27	0.02	14.88	0.01	14.81	0.03	0.120
73	BLHer	0.48966	LMC0515-6720D	53402.954	0.904	16.59	0.02	16.34	0.03	16.28	0.13	0.192
74	WVir	0.95368	LMC0514-6840A	52648.819	0.512	15.58	0.02	15.28	0.02	15.16	0.04	–0.051
75	RVTau	1.70059	LMC0518-6940C	52294.792	0.147	13.74	0.01	13.44	0.02	13.27	0.01	–
76	BLHer	0.32311	LMC0518-6820I	52657.914	0.487	17.19	0.03	16.77	0.03	16.64	0.09	–0.039
76	BLHer	0.32311	LMC0514-6820G	52660.786	0.852	17.51	0.05	17.14	0.07	17.05	0.16	–0.284
77	BLHer	0.08415	LMC0518-6940F	52294.841	0.534	17.66	0.04	17.52	0.08	17.23	0.23	–0.090
78	pWVir	0.82713	LMC0518-6920C	52303.770	0.294	15.30	0.02	14.88	0.02	14.73	0.03	–
79	WVir	1.17159	LMC0518-6820F	52657.863	0.117	15.13	0.02	14.71	0.02	14.60	0.02	0.283
80	RVTau	1.61190	LMC0518-6940C	52294.792	0.431	13.85	0.01	13.45	0.01	13.33	0.01	–
81	WVir	0.97679	LMC0518-7140C	52727.774	0.084	15.60	0.02	15.17	0.02	15.13	0.04	0.069
82	RVTau	1.54561	LMC0518-7140F	53356.035	0.488	14.62	0.01	14.14	0.01	13.93	0.02	–
83	pWVir	0.77580	LMC0518-7000I	52288.843	0.434	16.14	0.02	15.67	0.02	15.61	0.05	–
84	BLHer	0.24818	LMC0518-6920C	52303.770	0.675	17.24	0.06	16.85	0.07	16.83	0.17	–0.214
85	BLHer	0.53213	LMC0518-7120E	52761.750	0.704	16.86	0.03	16.59	0.06	16.39	0.09	–0.202
86	WVir	1.19991	LMC0518-6940E	52294.825	0.278	15.15	0.02	14.73	0.01	14.62	0.02	–0.156
87	WVir	0.71475	LMC0518-6940E	52294.825	0.118	16.22	0.02	15.82	0.02	15.70	0.06	0.106
88	BLHer	0.29020	LMC0518-7100H	52754.751	0.503	17.20	0.03	17.22	0.07	17.16	0.13	–0.022
89	BLHer	0.06718	LMC0518-6940B	53332.028	0.561	17.92	0.07	17.43	0.09	17.40	0.16	–0.189
90	BLHer	0.16995	LMC0518-6800E	52661.030	0.633	17.56	0.03	17.13	0.05	17.25	0.17	–0.195
91	RVTau	1.55327	LMC0518-6900D	52590.947	0.590	14.02	0.02	13.62	0.01	13.06	0.02	–
92	BLHer	0.41777	LMC0518-7000D	52288.914	0.702	17.22	0.04	16.91	0.06	16.91	0.18	–0.131
93	WVir	1.24534	LMC0518-7000G	52288.809	0.771	14.58	0.02	14.35	0.02	14.23	0.02	–0.212
94	WVir	0.92781	LMC0522-7000I	53421.909	0.708	15.72	0.02	15.30	0.03	15.25	0.05	–0.012
95	WVir	0.69898	LMC0522-6820F	52654.900	0.829	16.37	0.02	15.96	0.03	16.00	0.08	0.022
96	WVir	1.14382	LMC0522-6840C	52637.927	0.566	15.65	0.02	15.30	0.02	15.17	0.04	–0.339
97	WVir	1.02161	LMC0522-6920I	52301.918	0.620	15.65	0.02	15.27	0.02	15.18	0.03	–0.057

Table 4. –continued.

OGLE-ID	Type	log $P$	IRSF-Field		IRSF counterpart							$\delta_\phi$
			IRSF-Field	MJD(obs)	Phase	$J$	$E_J$	$H$	$E_H$	$K_s$	$E_K$	
98	pWVir	0.69668	LMC0522-7020I	52702.739	0.734	14.23	0.02	14.08	0.01	14.03	0.02	–
99	WVir	1.18996	LMC0522-6900F	52637.806	0.002	14.88	0.02	14.46	0.02	14.30	0.03	0.280
100	WVir	0.87105	LMC0522-7020F	53355.891	0.554	16.31	0.02	16.01	0.03	16.01	0.08	–0.187
100	WVir	0.87105	LMC0522-7020E	52700.891	0.411	16.13	0.02	15.79	0.02	15.91	0.06	–0.072
101	WVir	1.05761	LMC0522-6920H	52301.904	0.676	15.76	0.02	15.38	0.02	15.33	0.05	–0.302
102	BLHer	0.10244	LMC0522-7000E	52289.769	0.582	17.31	0.06	16.92	0.06	16.86	0.17	–0.226
103	WVir	1.11087	LMC0522-7020H	52701.758	0.478	15.55	0.02	15.12	0.02	15.00	0.03	–0.218
104	RVTau	1.39585	LMC0522-7000B	52287.914	0.982	14.14	0.02	13.74	0.03	13.41	0.02	0.172
105	BLHer	0.17298	LMC0522-7020E	52700.891	0.040	17.05	0.03	16.84	0.04	16.74	0.14	0.328
105	BLHer	0.17298	LMC0522-7020H	52701.758	0.622	17.63	0.07	17.13	0.07	16.92	0.21	–0.281
106	WVir	0.82651	LMC0522-6920B	52296.810	0.608	16.10	0.02	15.71	0.02	15.65	0.08	–0.029
107	BLHer	0.08248	LMC0522-6940E	52293.857	0.730	17.11	0.03	16.66	0.03	16.80	0.13	–0.066
108	RVTau	1.47728	LMC0522-6820H	52655.794	0.076	14.15	0.02	13.85	0.02	13.78	0.02	–
109	BLHer	0.15062	LMC0522-6940E	52293.857	0.525	18.44	0.10	17.93	0.10	–	–	–0.179
110	WVir	0.84994	LMC0522-6900H	52637.858	0.722	16.13	0.03	15.70	0.02	15.56	0.07	–0.010
111	WVir	0.87481	LMC0522-7100H	52760.825	0.717	15.97	0.02	15.58	0.02	15.45	0.03	–0.011
112	RVTau	1.59547	LMC0522-6920A	52296.794	0.608	13.64	0.01	13.30	0.01	13.23	0.02	–
113	BLHer	0.48932	LMC0522-6940G	52293.893	0.145	16.33	0.02	16.00	0.02	15.88	0.05	0.018
114	BLHer	0.03786	LMC0525-6820F	52681.761	0.833	17.39	0.04	16.99	0.04	16.77	0.18	–0.027
115	RVTau	1.39736	LMC0522-6940G	52293.893	0.950	14.56	0.01	14.17	0.01	14.09	0.02	0.293
116	BLHer	0.29373	LMC0526-6920C	52294.942	0.585	17.42	0.02	17.09	0.04	17.02	0.20	–0.154
117	WVir	0.82147	LMC0526-7100C	52939.119	0.767	16.08	0.02	15.70	0.01	15.63	0.03	–0.017
118	WVir	1.10376	LMC0525-6800B	52673.837	0.240	15.44	0.02	15.00	0.02	14.90	0.03	–0.195
118	WVir	1.10376	LMC0525-6820H	52683.781	0.023	15.12	0.03	14.74	0.02	14.58	0.03	0.297
119	RVTau	1.52924	LMC0526-7100I	52951.020	0.442	13.99	0.01	13.57	0.01	13.25	0.02	–
120	WVir	0.65887	LMC0525-6840B	52683.843	0.753	16.54	0.02	16.17	0.02	16.11	0.08	–0.077
121	BLHer	0.31416	LMC0526-7020E	52773.712	0.871	17.20	0.05	17.02	0.09	17.05	0.16	0.140
122	BLHer	0.18715	LMC0525-6840H	52683.954	0.007	17.46	0.04	17.14	0.06	17.10	0.22	0.186
122	BLHer	0.18715	LMC0525-6820B	52675.910	0.779	17.73	0.04	17.48	0.08	17.14	0.18	–0.093
124	BLHer	0.23927	LMC0525-6900G	53333.071	0.059	17.27	0.03	17.02	0.04	16.79	0.08	0.176
125	RVTau	1.51896	LMC0526-7140A	52959.955	0.407	14.35	0.01	13.92	0.01	13.87	0.03	–0.245
126	WVir	1.21290	LMC0526-7100G	53364.763	0.361	15.69	0.02	15.08	0.02	14.95	0.04	–0.370
127	WVir	1.10275	LMC0529-6920C	52362.833	0.694	15.56	0.02	15.15	0.02	15.04	0.03	–0.084
128	WVir	1.26700	LMC0530-7020I	52727.723	0.022	14.54	0.01	14.19	0.01	14.06	0.02	0.343
129	RVTau	1.79594	LMC0530-7000I	52338.892	0.062	13.65	0.02	13.32	0.01	13.22	0.02	–
130	BLHer	0.28885	LMC0530-7040F	52921.131	0.746	17.31	0.03	16.97	0.04	17.01	0.11	–0.293
131	BLHer	0.15029	LMC0529-6840H	52685.851	0.522	17.76	0.02	17.34	0.04	17.33	0.15	–0.186
132	pWVir	1.00077	LMC0530-7000H	52338.874	0.779	15.29	0.02	15.01	0.02	14.93	0.03	–
133	WVir	0.79809	LMC0530-7020B	52725.792	0.718	16.08	0.03	15.73	0.02	15.68	0.05	0.004
134	pWVir	0.61020	LMC0530-6940B	52338.925	0.466	15.90	0.02	15.61	0.02	15.46	0.05	–
135	RVTau	1.42361	LMC0529-6920H	52363.787	0.294	14.23	0.02	13.82	0.03	13.73	0.03	–0.115
136	BLHer	0.12157	LMC0530-6940H	52362.759	0.805	16.64	0.04	16.34	0.06	16.28	0.09	0.080
137	WVir	0.80362	LMC0530-6940E	52338.977	0.355	16.15	0.02	15.74	0.02	15.66	0.06	–0.019
138	BLHer	0.14414	LMC0529-6840A	52684.777	0.524	17.29	0.10	17.43	0.11	16.52	0.13	–0.175
138	BLHer	0.14414	LMC0529-6900G	52364.819	0.931	17.11	0.08	17.20	0.07	16.99	0.14	0.135
139	WVir	1.16969	LMC0529-6900A	52363.822	0.081	15.02	0.02	14.62	0.01	14.49	0.03	0.220
140	BLHer	0.26509	LMC0529-6920G	52363.769	0.331	17.16	0.03	16.78	0.05	16.83	0.13	0.025
141	BLHer	0.26078	LMC0531-7140E	52960.998	0.069	17.25	0.03	16.94	0.05	16.68	0.13	0.149
142	BLHer	0.24570	LMC0532-6800C	52765.718	0.313	16.79	0.09	15.74	0.06	15.62	0.12	0.034
143	WVir	1.16347	LMC0529-6920G	52363.769	0.569	15.57	0.02	15.27	0.02	15.17	0.04	–0.401

Table 4. –continued.

OGLE-ID	Type	log $P$	IRSF-Field		IRSF counterpart							$\delta_\phi$
			IRSF-Field	MJD(obs)	Phase	$J$	$E_J$	$H$	$E_H$	$K_s$	$E_K$	
143	WVir	1.16347	LMC0533-6920I	53331.899	0.014	14.86	0.03	14.52	0.02	14.44	0.02	0.332
144	BLHer	0.28723	LMC0533-6900I	52286.935	0.371	16.73	0.05	–	–	16.73	0.11	–0.124
145	BLHer	0.52340	LMC0533-6900F	52283.877	0.087	16.32	0.02	16.15	0.02	16.11	0.07	0.067
146	WVir	1.00344	LMC0533-6840C	52687.758	0.228	15.63	0.02	15.25	0.01	15.12	0.03	0.006
146	WVir	1.00344	LMC0533-6900I	52286.935	0.463	15.88	0.01	15.51	0.02	15.35	0.03	–0.111
147	RVTau	1.67021	LMC0533-6920I	53331.899	0.585	13.49	0.02	13.15	0.01	12.95	0.01	–
148	BLHer	0.42679	LMC0533-6920C	52969.042	0.572	17.13	0.02	16.85	0.03	16.66	0.07	–0.292
148	BLHer	0.42679	LMC0533-6940I	52226.973	0.824	16.84	0.02	16.67	0.04	16.57	0.10	0.110
149	RVTau	1.62819	LMC0533-6940H	52218.098	0.615	13.67	0.01	13.36	0.01	13.26	0.02	–
150	WVir	0.73981	LMC0534-7100F	52563.936	0.352	15.77	0.02	15.53	0.02	15.38	0.04	–0.021
151	WVir	0.89693	LMC0534-7000D	52314.930	0.863	15.87	0.02	15.46	0.02	15.39	0.04	0.040
152	WVir	0.96918	LMC0534-7000D	52314.930	0.938	15.55	0.02	15.15	0.02	15.05	0.03	0.180
153	BLHer	0.07010	LMC0534-7100B	52563.994	0.623	16.55	0.03	16.47	0.03	16.35	0.07	–0.048
154	pWVir	0.87955	LMC0534-7100G	52563.922	0.498	15.04	0.02	14.86	0.01	14.77	0.03	–
155	WVir	0.83871	LMC0534-7040A	52335.748	0.926	15.70	0.04	15.23	0.05	15.12	0.05	0.049
156	WVir	1.18714	LMC0534-7100D	52563.965	0.886	15.03	0.02	14.67	0.01	14.55	0.02	0.267
157	WVir	1.15639	LMC0537-6920C	52958.909	0.289	15.36	0.01	14.90	0.01	14.78	0.02	–0.173
158	WVir	0.85365	LMC0536-6820B	53364.839	0.694	16.12	0.01	15.73	0.02	15.69	0.06	–0.011
159	WVir	0.82122	LMC0537-6940H	53019.932	0.464	16.11	0.01	15.72	0.02	15.59	0.03	–0.038
160	BLHer	0.24469	LMC0538-7100I	52514.153	0.627	17.49	0.03	17.11	0.06	17.05	0.09	–0.243
161	WVir	0.93107	LMC0539-7120I	53334.830	0.376	15.18	0.01	14.71	0.02	14.59	0.03	–0.045
162	RVTau	1.48279	LMC0537-7000H	52314.847	0.942	14.12	0.02	13.69	0.02	13.53	0.02	–
163	BLHer	0.22881	LMC0540-6820F	53355.951	0.379	17.12	0.02	16.73	0.03	16.74	0.12	0.041
164	pWVir	0.92918	LMC0538-7020E	52315.872	0.174	15.25	0.02	14.82	0.02	14.50	0.02	–
165	BLHer	0.09371	LMC0537-6920A	52954.932	0.736	18.09	0.04	17.83	0.09	–	–	–0.098
166	BLHer	0.32441	LMC0537-6940A	53331.928	0.098	16.23	0.02	15.88	0.02	15.79	0.03	0.092
167	BLHer	0.36395	LMC0541-6940F	53276.054	0.232	17.01	0.02	16.65	0.03	16.49	0.05	0.068
168	WVir	1.19585	LMC0540-6820E	53355.939	0.295	15.22	0.01	14.74	0.01	14.62	0.02	–0.199
169	RVTau	1.49074	LMC0539-7120D	53334.783	0.534	14.60	0.02	14.14	0.01	14.01	0.03	–0.451
170	WVir	0.88553	LMC0540-6840B	52691.787	0.524	16.05	0.02	15.61	0.02	15.51	0.04	–0.071
171	BLHer	0.19166	LMC0541-7000F	52306.813	0.553	17.44	0.05	17.16	0.08	17.03	0.20	–0.141
172	WVir	1.05002	LMC0541-7000C	52305.912	0.382	15.58	0.02	15.16	0.02	15.02	0.04	–0.138
173	WVir	0.61783	LMC0541-7000I	52306.863	0.531	17.15	0.03	16.55	0.06	16.34	0.11	–0.100
174	RVTau	1.67042	LMC0541-6940F	53276.054	0.703	13.16	0.02	12.73	0.01	12.11	0.01	–
175	WVir	0.96968	LMC0540-6840H	52691.886	0.215	15.74	0.02	15.31	0.02	15.18	0.03	0.011
176	WVir	0.90253	LMC0539-6800D	52683.885	0.226	15.77	0.02	15.37	0.02	15.32	0.04	0.007
177	WVir	1.17713	LMC0541-6920H	52528.126	0.298	15.33	0.01	14.83	0.01	14.67	0.01	–0.167
178	WVir	1.08680	LMC0542-7020B	52306.897	0.456	15.71	0.02	15.28	0.02	15.18	0.03	–0.144
179	WVir	0.90580	LMC0541-7000D	52306.767	0.133	15.91	0.02	15.50	0.02	15.36	0.04	0.047
180	RVTau	1.49131	LMC0544-6840H	52685.857	0.394	14.03	0.02	13.57	0.01	13.08	0.02	–
181	pWVir	0.85809	LMC0542-7040D	52312.856	0.308	15.57	0.02	15.35	0.02	15.17	0.03	–
182	WVir	0.91521	LMC0542-7040D	52312.856	0.191	15.52	0.01	15.21	0.01	15.06	0.02	0.132
183	WVir	0.81356	LMC0545-6940B	52293.036	0.909	16.39	0.02	15.88	0.03	15.80	0.05	0.047
184	WVir	1.17145	LMC0545-6940H	53427.831	0.446	15.84	0.02	15.29	0.02	15.17	0.04	–0.309
185	WVir	1.10341	LMC0545-7000H	52305.849	0.008	13.60	0.01	13.12	0.02	12.97	0.02	0.066
186	WVir	1.21383	LMC0544-6840A	52684.782	0.109	14.79	0.02	14.45	0.01	14.37	0.02	0.309
187	BLHer	0.38102	LMC0545-6940A	53423.853	0.068	16.98	0.03	16.73	0.07	16.72	0.15	0.249
188	BLHer	0.02091	LMC0545-7000D	52303.874	0.885	17.60	0.06	17.54	0.09	–	–	0.061
189	BLHer	0.11649	LMC0547-6840B	53722.781	0.868	17.50	0.05	17.32	0.08	16.96	0.16	0.140
190	RVTau	1.58390	LMC0549-6940G	53491.741	0.735	13.61	0.02	13.28	0.01	13.19	0.03	–
191	RVTau	1.53586	LMC0553-7000I	52362.918	0.173	13.60	0.02	13.27	0.01	13.05	0.02	–
192	RVTau	1.41820	LMC0554-7020E	52345.935	0.299	14.66	0.02	14.27	0.02	14.16	0.02	–0.183
193	WVir	0.84540	LMC0557-7200I	52313.831	0.794	15.96	0.02	15.60	0.02	15.48	0.05	0.030